iScience, Volume *25*

Supplemental information

Role of pericytes in the development of cerebral cavernous malformations

Zifeng Dai, Jingwei Li, Ying Li, Rui Wang, Huili Yan, Ziyu Xiong, Shiting Wu, Xi Yang, Dongbo Lu, Dongdong Zhang, Guofu Li, Yuwen Wang, Chunyang Men, Wenzhong Du, Xiangjian Zheng, and Changbin Shi

Supplemental figures and figure legends

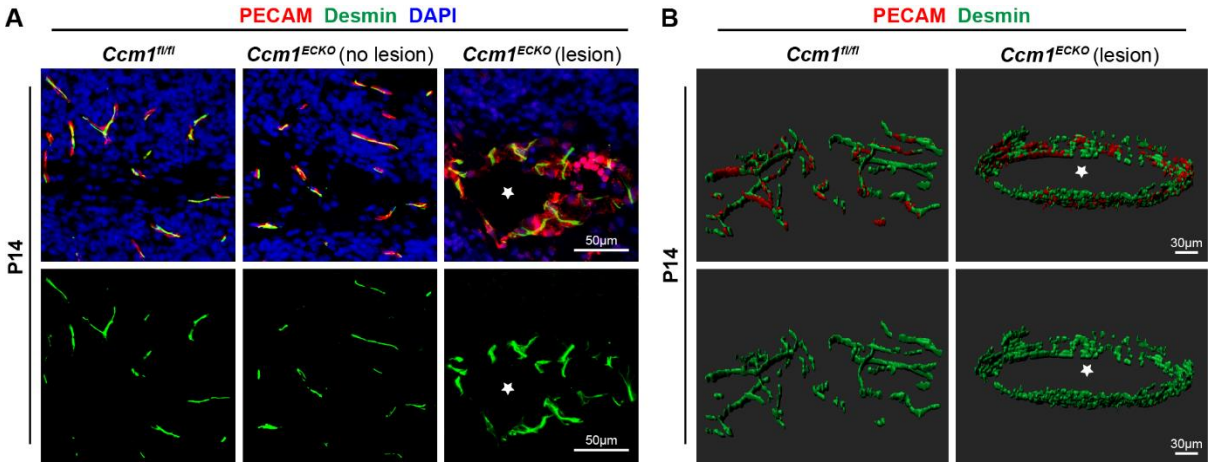

Figure S1. Pericytes were reshaped in CCM lesions, related to Figure 4. A-B Representative IF images of desmin and PECAM in normal vessels and CCM lesions in 2D images (**A**) and 3D reconstructive images (**B**). The shape of pericytes became abnormal and had more complex processes in CCM lesions (**A**). Representative images of CCM lesions were indicated by asterisks. Scale bar: 50 μm in **A;** 30 μm in **B**.

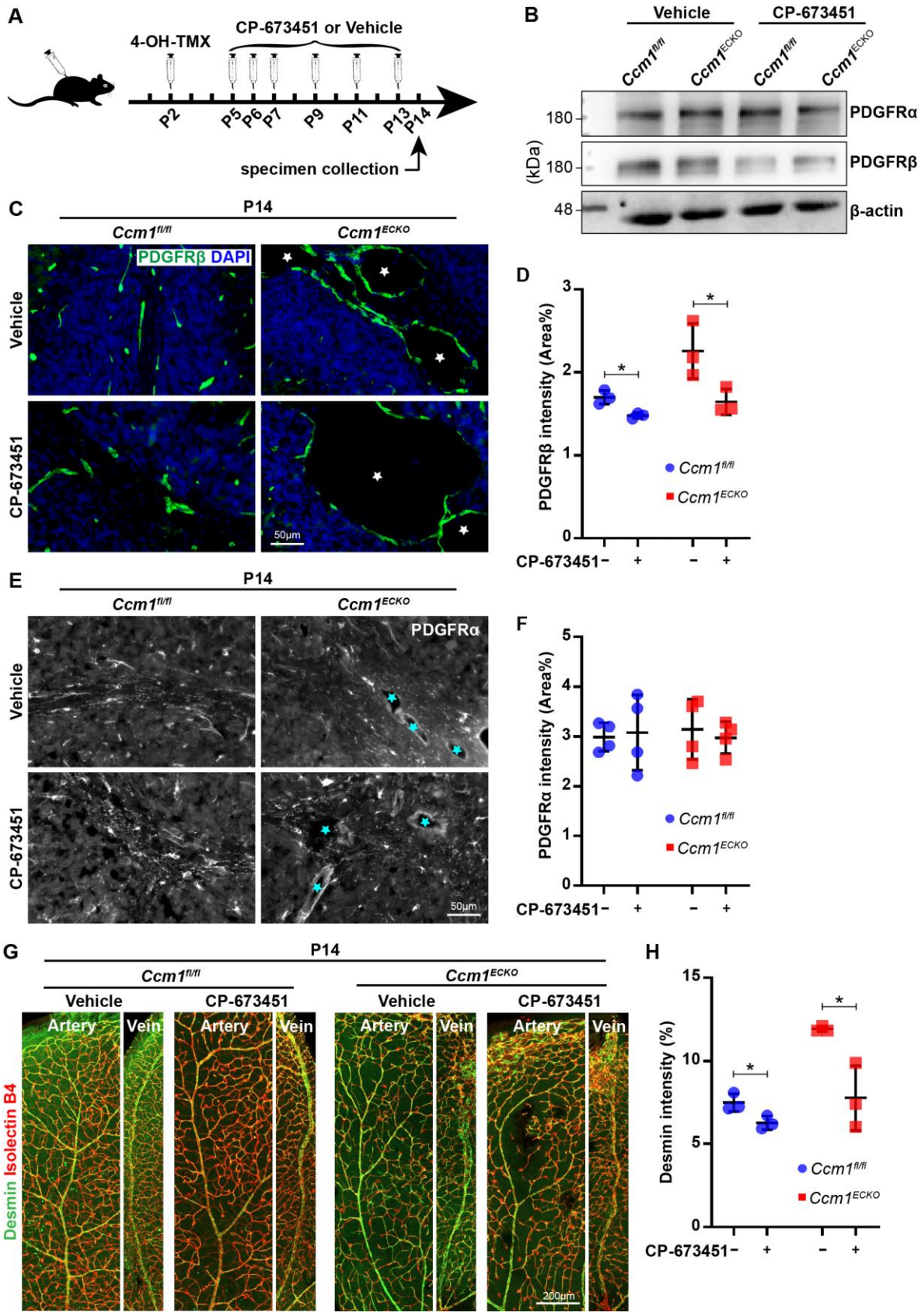

Figure S2. Pericyte coverage was decreased in CP-673451-treated mice, related to Figure 2. A
The schematic diagram depicts the experimental schedule during which mice are administered

CP-673451 or vehicle from P5–P13 and brain samples are collected at P14. **B** PDGFRβ and PDGFRα were determined by WB with respective antibodies. **C-D** Representative images of staining for PDGFRβ from mice treated with vehicle or CP-673451. Quantification results showed CP-673451 decreased the expression of PDGFRβ. **E-F** Representative images of PDGFRα staining were showed. Quantification results showed CP-673451 did not have a significant effect on the expression of PDGFRα. **G-H** Representative confocal microscopy images of retinas in mice treated with vehicle or CP-673451. Pericyte coverage became sparse and the expression of desmin was downregulated in CP-673451-treated mice. Cerebellar CCM lesions were indicated by asterisks. Data are presented as mean ± SD. Scale bar: 50 μm in **C** and **E;** 200 μm in **G**. *$P < 0.05$, unpaired Student's *t*-test for **C, G** and **K**.

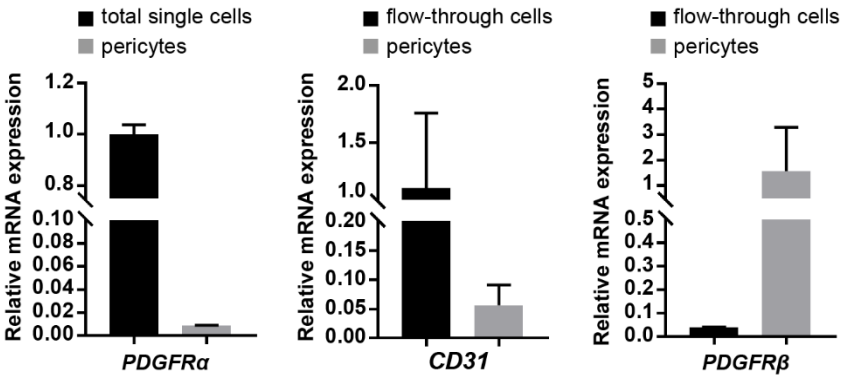

Figure S3. Pericytes showed a good enrichment ratio, related to Figure 3. Pericytes were purified by the anti-PDGFRβ antibody. Relative mRNA expression level (fold change) of *CD31*, *PDGFRα*, and *PDGFRβ* in pericytes and total single cells or flow-through cells. Data are presented as mean ± SD.

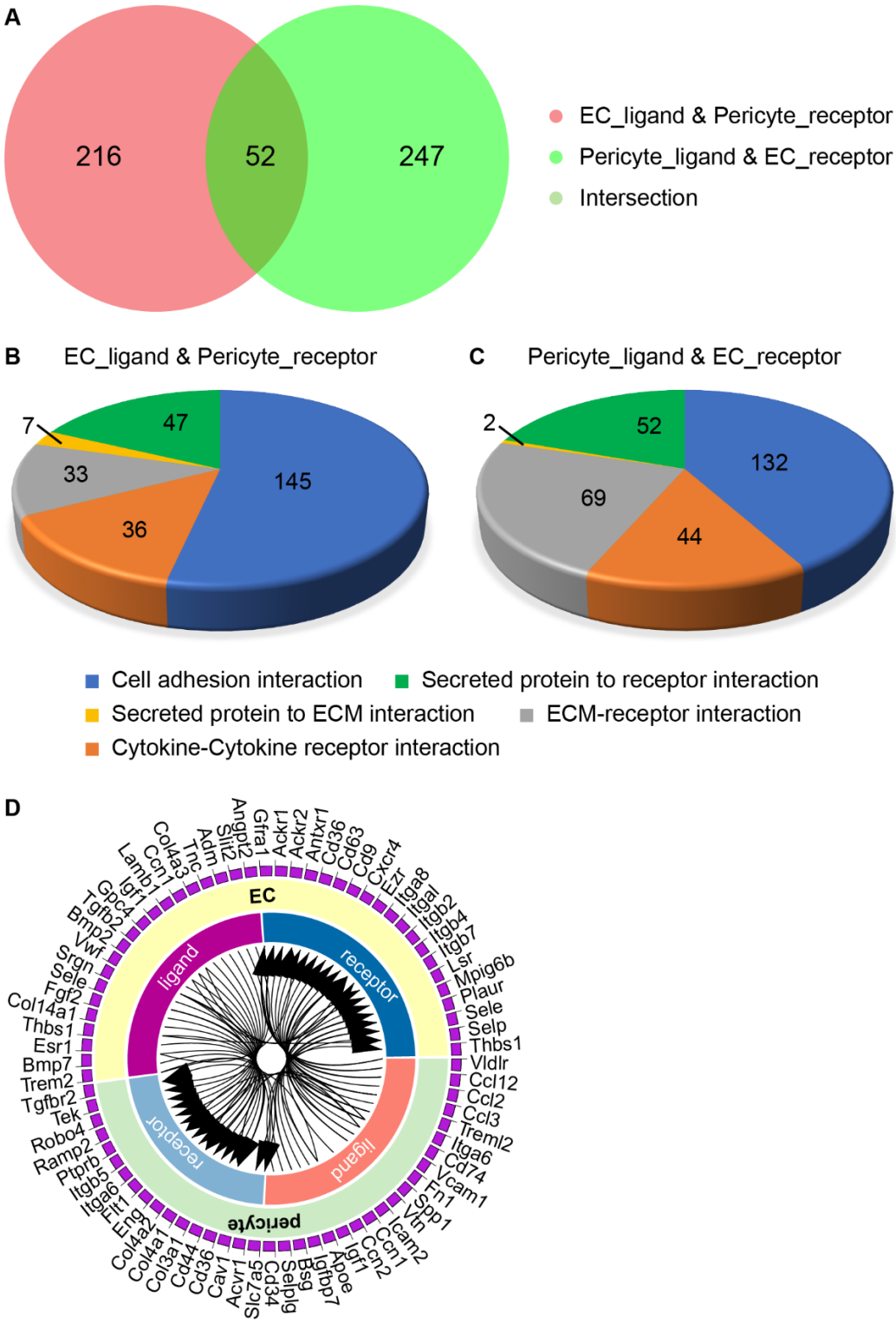

Figure S4. Ligand-receptor interactions between pericytes and ECs in CCM lesions, related to Figure 3. A 515 ligand/receptor complexes were involved in the crosstalk between pericytes and ECs in CCM lesions. **B-C** Category distributions of ligand/receptor interactions between pericytes and ECs. **D** Chord plot summarizing the significant pairwise interaction of the ligand genes and receptor genes in pericytes and ECs.

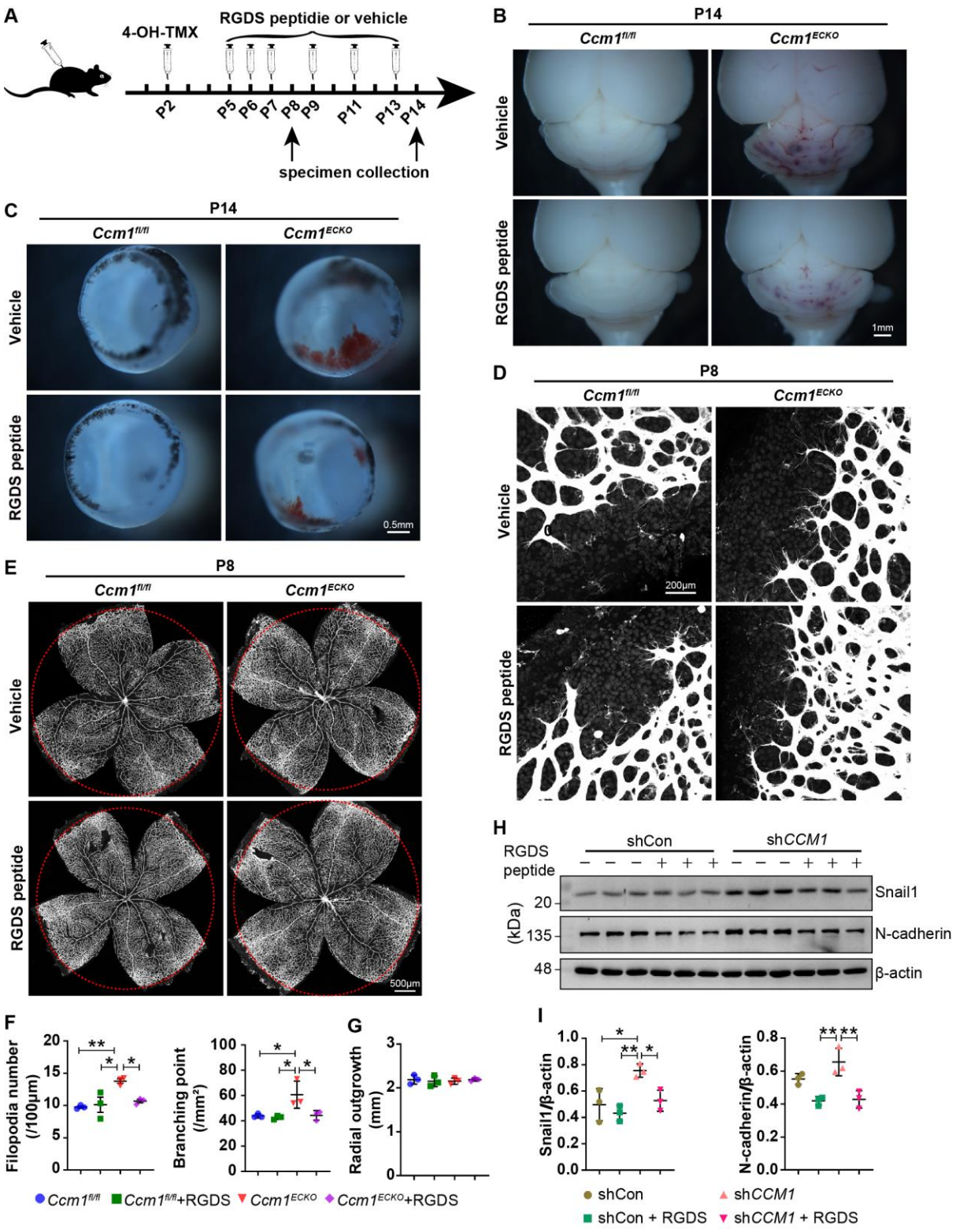

Figure S5. RGDS peptide decreased the number of retinal filopodia and downregulated the expression of EndMT-related markers, related to Figure 5. A The schematic diagram depicts the experimental schedule during which the mice were administered RGDS peptide or vehicle from P5–P13. Brain samples were collected at P8 and P14. **B-C** The gross anatomical images of cerebella (**B**) and retinas (**C**) at P14. **D** Representative confocal microscopy images of retinal filopodia at P8. **E**

Representative confocal microscopy images of radial outgrowth of the retina at P8. The red dotted circles indicated the boundary of radial outgrowth. **F** Quantification of filopodia density (numbers/100 μm) and vascular branching point density in (**D**). **G** Quantification of radial outgrowth in (**E**). **H-I** WB analysis of indicated parameters in sh*CCM1* or shCon HUVECs treated with or without RGDS peptide for 24 h. Data are presented as mean ± SD. Scale bar: 1 mm in **B**; 0.5 mm in **C**; 200 μm in **D**; 500 μm in **E**. *$P < 0.05$, **$P < 0.01$, one-way ANOVA with Tukey's *post-hoc* test for **F**, **G**, and **I**.

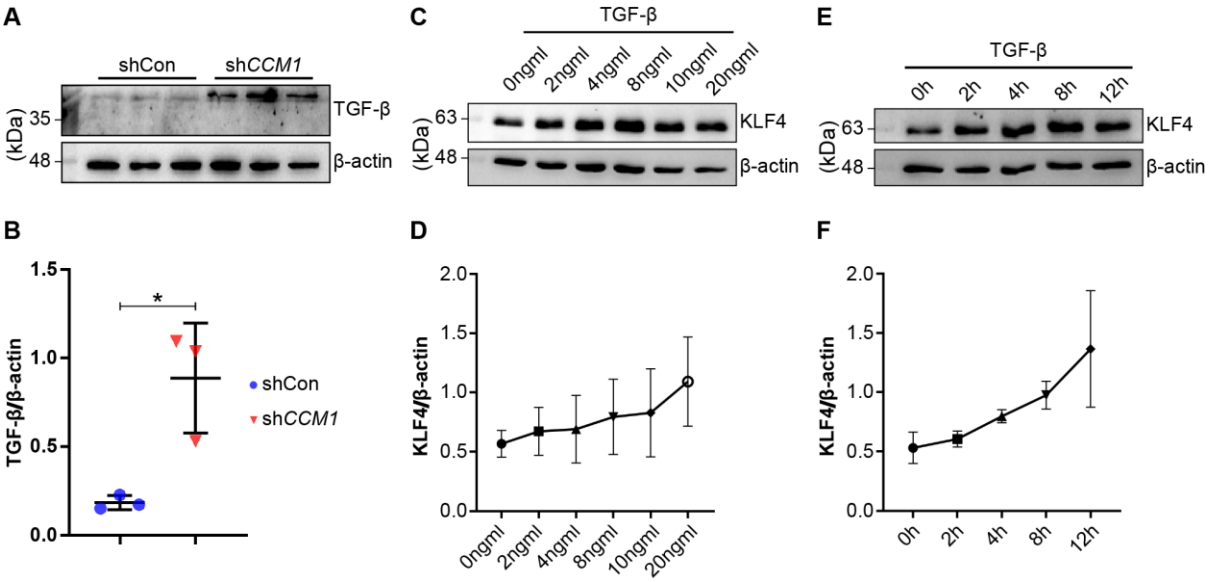

Figure S6. TGF-β treatment increased the expression of KLF4 in pericytes, related to Figure 6. **A-B** WB analysis showed that HUVECs transfected with sh*CCM1* resulted in increased expression of TGF-β. **C-F** WB analysis of KLF4 expression in HBVPs treated with TGF-β. Quantitative results showed an increased expression of KLF4 in HBVPs treated with TGF-β in a time- and dose-dependent manner (n = 3 per group). Data are presented as mean ± SD. *P < 0.05, unpaired Student's t-test for **B**.

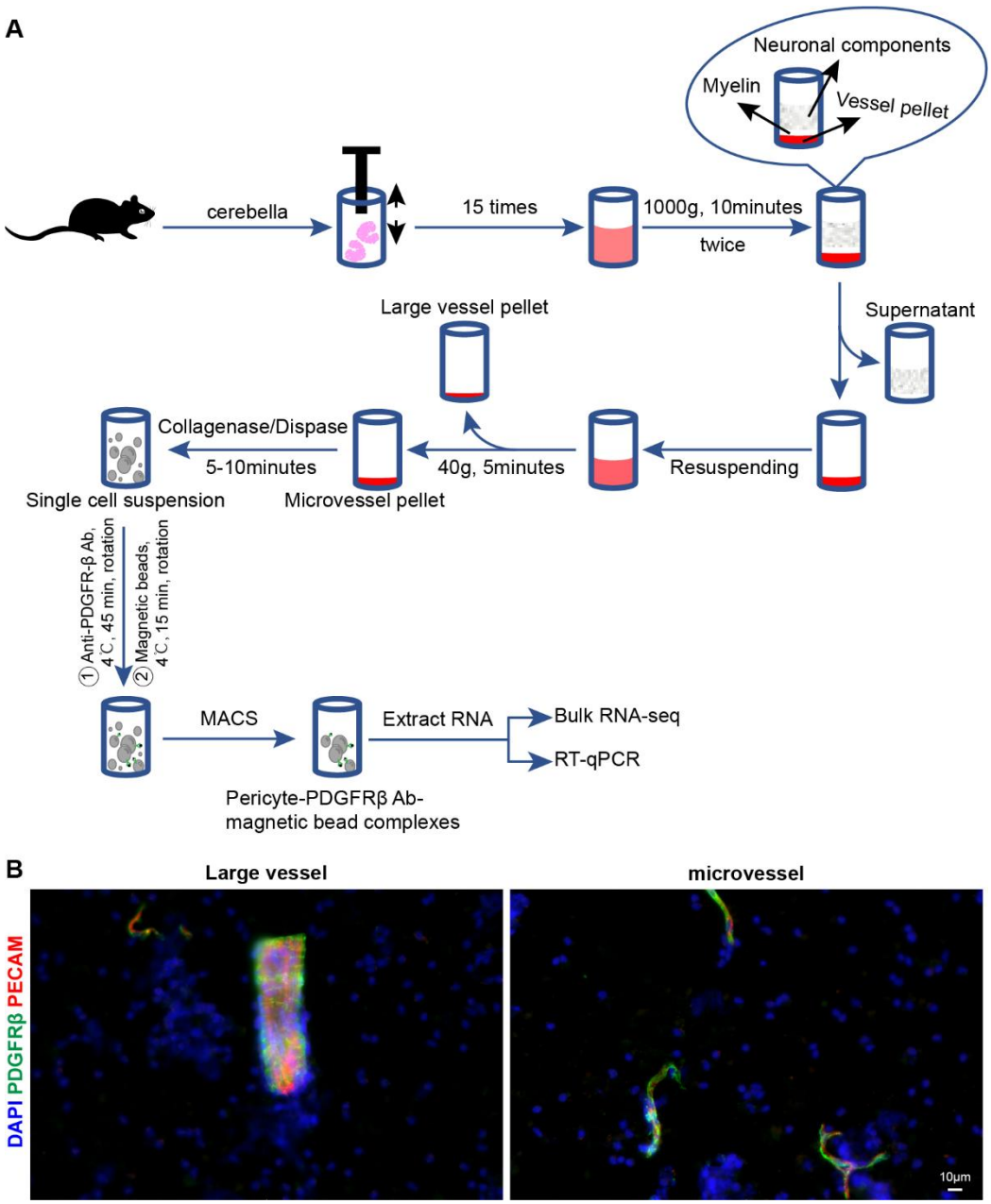

Figure S7. The isolation of pericytes and microvessels in cerebella, related to STAR Methods. A Flow diagram for the isolation of pericytes in cerebella. **B** The representative IF staining images of large vessels (> 10 μm) and microvessels (≤ 10 μm). IF staining demonstrated that perivascular cells around large vessels have flattened and few cytoplasmic processes, whereas pericytes around microvessels are distinctly protruding with several processes encircling the endothelium. Scale bar: 10 μm.

Table S2. Raw data including exactly animal numbers in each group (for different experiments), related to SRAR Methods.

Experiment	Age of mouse	*Ccm1*$^{fl/fl}$	*Ccm1*^{ECKO}	*Ccm1*$^{fl/fl}$ + CP-673451	*Ccm1*^{ECKO} + CP-673451	*Ccm1*$^{fl/fl}$ + RGDS peptide	*Ccm1*^{ECKO} + RGDS peptide
IF staining	p7	4	4				
	p14	3	3				
	p28	3	3				
WB	p14	3	3				
WB in mice treated with CP-673451	p14	3	3	3	3		
IF, H&E or retinal whole-mount staining in mice treated with CP-673451	p14	5	5	5	5		
H&E or retinal whole-mount staining in mice treated with RGDS	p14	5	5			5	5
TEM	p7	3	4				
	p14	3	3				
	p28	5	3				
RNA-seq	p14	3	3				
RT-qPCR	p14	3	3				
retinal whole-mount staining in mice treated with RGDS peptide	p8	3	3			3	3
Total		46	45	8	8	8	8

(IF = immunofluorescence, WB = Western blotting, H&E = hematoxylin-eosin, TEM = transmission electron microscope, RNA-seq = RNA-sequencing, RT-qPCR = real-time quantitative polymerase chain reaction)